Wasit Journal for Pure Science

Journal Homepage: https://wjps.uowasit.edu.iq/index.php/wjps/index

e-ISSN: 2790-5241 p-ISSN: 2790-5233

Biosynthesis of Iron Oxide Nanoparticles by Fungi Beauveria Bassiania and Study of their Structural and Optical Properties

Karrar Talib Nima Badr[1]* and Muneer Hlail Jaduaa Alzubaidy[2]

[1,2]Department of Physics, College of Science, Wasit University, IRAQ

*Corresponding Author: Karar Talib Nima

DOI: https://doi.org/10.31185/wjps.513

Received 22 July 2024; Accepted 12 September 2024; Available online 30 September 2024

ABSTRACT: Iron oxide nanoparticles were synthesized using a biological approach using the *Beauveria bassiana fungus*. The synthesized nanoparticles were characterized using X-ray diffraction (XRD), scanning analysis (SEM), and atomic energy microscope (AFM). The iron oxide NPs in an average grain size of ~ 39 nm. The topography and features of the surface show that there are ripples distributed regularly and homogeneously on the surface and that the deposited film is regular. The optical properties of iron oxide NPs were studied using UV/Vis spectroscopy, and it was found that the absorbance gradually decreases as we approach the visible light region, starting from its peak at short wavelengths, where the surface plasmon resonance was recorded, which showed the absorbance at the UV wavelength at (282 nm), and the absorbance is at its maximum at high energies (short wavelengths), then decreases with increasing wavelength to reach its lowest value in the visible region of the spectrum, and for this reason the absorbance decreases with increasing wavelength, where the energy gap value is (2.5 electron volts). The FTIR spectrum showed functional groups have been recorded in a range $(400-3900)cm^{-1}$These results confirm the presence of the fungal extract belonging to the fungus Beauveria bassiana. The vibrations in the phenolic compounds are responsible for the interaction process with the salts of the basic materials used in the preparation.

Keywords: *Beauveria bassiana* fungus, iron oxide NPs, topography, optical properties, energy gap, crystal size، Bio-synthesized

1. INTRODUCTION

Nanomaterials are characterized by their unique properties. It is a term that describes materials in terms of the atomic or molecular scale and their dimensions are measured in nanometers, which is a part of (one thousandth of a micrometer) or a part of (one millionth of a millimeter). Which states that nanomaterials are those materials whose linear dimensions are less than (100nm) and are usually between (1 - 100 nm) [1]. This clearly affects the physical and chemical properties of nanomaterials, especially color, magnetic and mechanical properties [2]. Nanotechnology has great benefits on a wide scale, as nanomaterials have the ability to improve the environment by creating new solutions to environmental problems, for example, applications of nanomaterials to detect, prevent and remove pollutants [3]. Nanotechnology is a clean and environmentally friendly industrial process [4]. Nanotechnology has benefits such as early diagnosis, treatment and prevention of cancer and other diseases [5]. Or continuous health monitoring and treatment using small and cheap sensors [6]. The rapid growth of nanotechnology industry and its increasing applications will certainly increase the concentration of nanomaterials in the environment, with the potential to increase human and environmental exposure [7]. The human body is exposed to NPs through four possible routes such as inhalation of airborne nanoparticles, ingestion of food additives, injection of engineered nanoparticles, and skin penetration through skin contact [8]. At present, green synthesis technology for the production of metal oxide nanoparticles has been rapidly developed. Many elements of nature have been used as reagents for the synthesis of nanoparticles. These reagents include microorganisms, such as fungi, bacteria, and yeast; plant extract sources, such as roots, fruits, leaves, flowers, stems, and peels; and pure biodegradable materials, such as proteins, vitamins, and enzymes [9]. The use of microorganisms and biodegradable materials is not as cost-effective as the use of plant extract; it usually takes a long time to screen and cultivate the microbes; and it is also difficult to manufacture nanoparticles with controlled size and shape using microorganisms. Moreover, the mechanism by which nanoparticles are formed using this approach is currently unclear [10].

2. MATERIALS AND METHODS

2.1. Preparation of broth and culture of *Beauveria bassiana fungus*

Beauveria bassiana was grown according to the following steps:

1- Cucumber pieces were cut with a thickness not exceeding 3 mm and a diameter of 2 cm, and a weight of 20 g (± 5).

2- Prepare the sugar solution by dissolving 10 g per 100 ml at a temperature of (60℃) for half an hour.

3- Add 2 g of *Beauveria bassiana* powder equally to 8 pieces of cucumber. As shown in the figure (1).

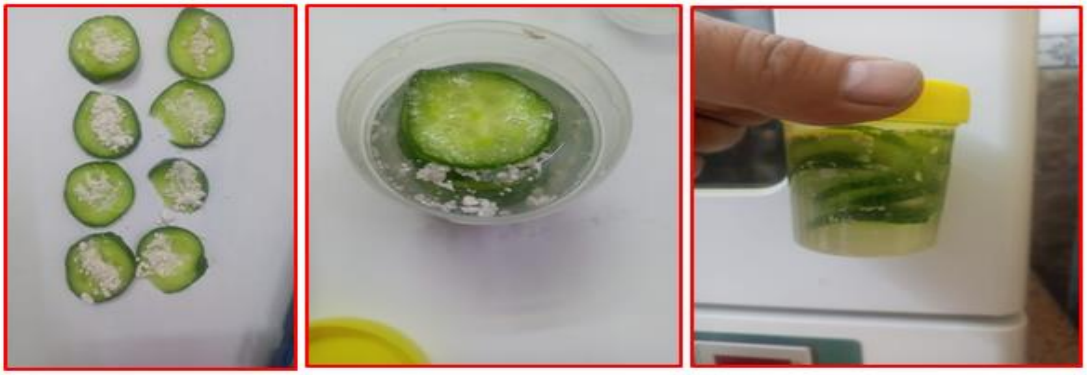

Figure 1. Method for preparing Beauveria bassiana mushroom extract

4- All cucumber pieces were collected and placed in a sugar solution at a concentration of 1 g per 100 ml.

5- The fungal extract was placed in a container at a temperature of 20 degrees Celsius for 14 days.

6- Purification was carried out at a rate of (four times) to obtain the extract.

2.2. Synthesis of nano-iron oxide particles

Prepare a solution FeSO_4(H_2O)$_7$

Ferrous sulfate heptahydrate, also known as iron sulfate, is a blue crystal with a positive alternating crystal system and a typical closed hexagonal structure. It is an inorganic compound and the molecular weight is 278.0146 g/mol, and thus the molar mass is 278.0146 g/mol. 2.780 gm was taken at a molar concentration of (0.1) and dissolved in (100 ml) of deionized water in a glass flask and heated for (30) minutes at a temperature of (60°C) using a magnetic stirrer and then mixed with (10 ml) of the fungal extract solution which was added gradually and at the same temperature to the prepared mineral salt solution and left to react until the color changed to light yellow as shown in Figure (2). The enzymes, proteins and other compounds present in the fungal fluid act as reducing agents and are responsible for converting iron salts into nanoparticles of iron oxide. To calculate the molecular weight of iron sulfate, the weight was calculated using the equation

$$M = \frac{wt}{Mwt} \times \frac{1000}{V} \dots\dots\dots\dots\dots (1)$$

Where: M: Molar concentration Wt: Weight of the materials used Mwt: Molecular, weight of materials (g / mole) and V: Volume of distilled.

Where the molarity is equal to 0.1 and the molecular weight of the solution (FeSO_4(H_2O)7 is g/mol and the required volume is equal to 100. By applying the equation, the weight value is equal to 2.780 g. Figure (2) shows the nano-iron oxide solution.

Figure (2) shows a figure showing the nano-iron oxide solution.

2.3. X-ray diffraction of FeNPs

Samples of iron nanoparticles coated by spin deposition on glass slides were characterized by an X-ray diffraction system (Aeris research edition) using Cu Kα radiation. In a scattering range (2Θ) from 20 - 80 degrees.

2.4. Ultraviolet-visible (UV-VIS) spectroscopy of FeNPs

By ultraviolet and visible spectroscopy (UV-VIS). Iron concentrations were monitored by UV-VIS spectrometry of the reaction medium for time periods from 24 h to 120 h and was recorded at 420 nm using a UV-VIS spectrometer.

2.5. Scanning electron microscopy (SEM) analyses of FeNPs

SEM measurements were done with Panalytical company SEM. SEM provide further insight into the morphological details of the iron nanoparticles.

2.6. Fourier transform infrared spectroscopy (FTIR) of FeNPs

FTIR spectra of FeNPs were obtained with a Fourier transform infrared spectroscopy (FTIR). The FeNPs substance was characterized in stages at a spectrum range of (1550-1650) cm^{-1}.

2.7. Atomic force microscopy (AFM) measurements of FeNPs

The surface topography of the nanoscale iron samples was studied using an atomic force microscope (Model TT-2) in order to obtain the characteristics of the iron particles and know the distribution of these particles on the surface, as well as other important information

3. RESULTS AND DISCUSSION

3.1. Biosynthesis of Iron nanoparticles

Iron nanoparticle biosynthesis was observed by all *B. bassiana* isolates in the culture supernatant treated with $FeSO_4(H_2O)_7$. the color changed to light yellow as shown in Figure (2).

3.2. X-Ray Diffraction Measurements

The X-ray diffraction analysis of the sample, biosynthesized using the fungus *Beauveria bassiana*, reveals a nanocrystalline structure with three distinct peaks at 2θ angles of 25.68°, 28.48°, and 35.35°. These peaks correspond to d-spacings of 1.81 Å, 2.006 Å, and 2.47 Å respectively. The crystallite sizes, calculated using the Scherrer equation, vary significantly across these planes, ranging from 0.29 nm to 3.87 nm, confirming the nanostructure of the material. The Full Width at Half Maximum (FWHM) values for these peaks are 0.031°, 0.035°, and 0.043°, indicating varying degrees of peak broadening. Notably, the dislocation density shows considerable variation, with an exceptionally high value of 11506.02 lines/m² for the peak at 28.48°, suggesting a higher concentration of defects in this particular crystal plane. The microstrain values, which indicate lattice distortions, range from 0.65 to 10.48 $lines^{-2}.m^{-4}$, with the highest strain observed for the peak at 35.35°. These results collectively provide valuable insights into the crystal structure, size distribution, and defect concentration of the biosynthesized sample, which can be crucial for understanding and optimizing its material properties.The results are tabulated in Table (1).

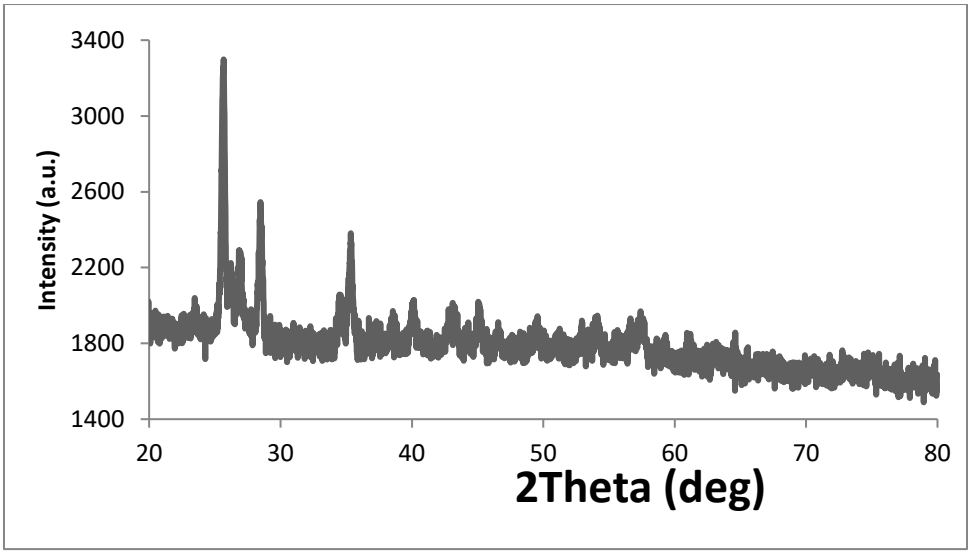

Figure (3): XRD patterns of iron nanoparticles biosynthesized by *B. bassiana*.

Table (1): shows the synthetic properties of a substance $FeSO_4(H_2O)_7$.

$2\theta°$	FWHM	FWHM (deg)	D nm	δ lines/m^2	$\eta * 10^{-3}$ lines^{-2}.m^{-4}
25.68	1.81	0.031	3.87	66.48	6.99
28.48	2.006	0.035	0.29	11506.02	0.65
35.35	2.47	0.043	3.11	103.06	10.48

The crystal size and inter distances were calculated as shown in Table (1). the method is suitable for preparing iron oxide, with a slight difference in the shape of the spectrum of reflected rays, which is due to the effect of the extract. The average crystal size (D_{ave}) was calculated according to Schreier's equation:

$$D_{ave} = \frac{0.94\lambda}{\beta\cos\Theta} \qquad (1)$$

where: β - represents the full width at half maximum in the unit (radian) θ - represents the Braque diffraction angle. The indicator of the quality of the crystal is the number of dislocation lines that cross a unit area in the crystal, which represents the total length of all the dislocation lines and the size of the crystal, which is given by the following relationship [11].

$$\delta = \frac{1}{D_{ave^2}} \qquad (2)$$

where: (δ) the density of dislocations in units. Dislocation Lines / (nm)² .The thin film may suffer from microstress and dislocation in its structure due to the heat treatment process accompanying the deposition process on the substrate, as the microstress is calculated through the following relationship:

$$\eta = \frac{\beta \cos\Theta}{(4)} \qquad (3)$$

where: (η) Microstress is measured in units (m^{-4} . $Lines^{-2}$)

3.3. Atomic force microscopy results

The topography of the prepared membrane surfaces deposited on glass substrates was studied using spin coater method at a temperature of (60℃). The atomic force microscope (AFM) was used, which is characterized by its high ability to image and analyze these surfaces and provide very accurate information about the distribution of particles and about the surface roughness values (Surface Roughness) depending on the square root of the mean square of the roughness (RMS), as is clear from the scanning process of the surface structures of the prepared membrane shown in the figure (4) We notice that there are ripples distributed regularly and homogeneously on the surface and that the deposited film is regular and that the roughness rate reaches (12.062 nm) and that the distances separating those peaks, which represent the mean free path (6.720 nm), as shown in Table (2).

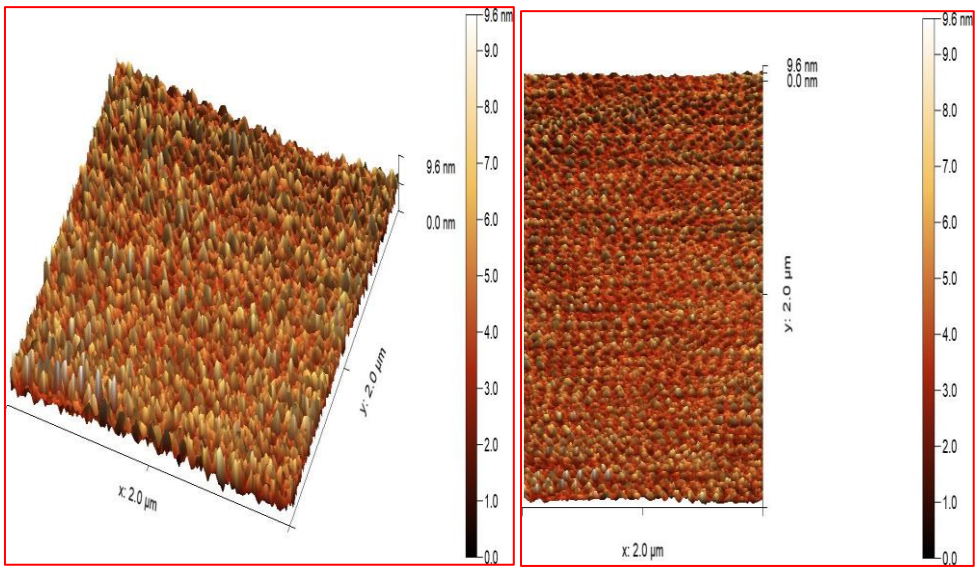

Figure (4): two and three-dimension images, mediated by the atomic power microscope of the sample

Table (2): Values of surface roughness rate and square root values of the mean roughness square and grain size rate according to the AFM measurements of $FeSO_4(H_2O)_7$

Sample	Average Grain size (nm)	Roughness average (nm)	Root mean square (nm)
$FeSO_4(H_2O)_7$	38.6377	12.06	6.720

3.4. SEM analyses of FeNPs

Figure (5) shows SEM images of the bio-prepared membrane that was deposited on glass substrates by spin coater method at a temperature of (60°C). The SEM images confirm the different morphology of these nanoparticles, as the morphology of these particles is in the form of irregular and dispersed particles with some homogeneous crystal structures and shapes that were formed by the fungal extract in the micro state. When the image is enlarged in the nano state, we will notice that the particles are well separated from each other, while most of them are present in a clumped form resembling mushroom structures and consisting of building units that were observed with average grain sizes ranging from 49.58 nm to 68.11 nm. The crystal size can be calculated as previously explained, where a measurement was taken for the size of a single crystal of 4 mm, and by applying the previous equation, we get 500 nm.

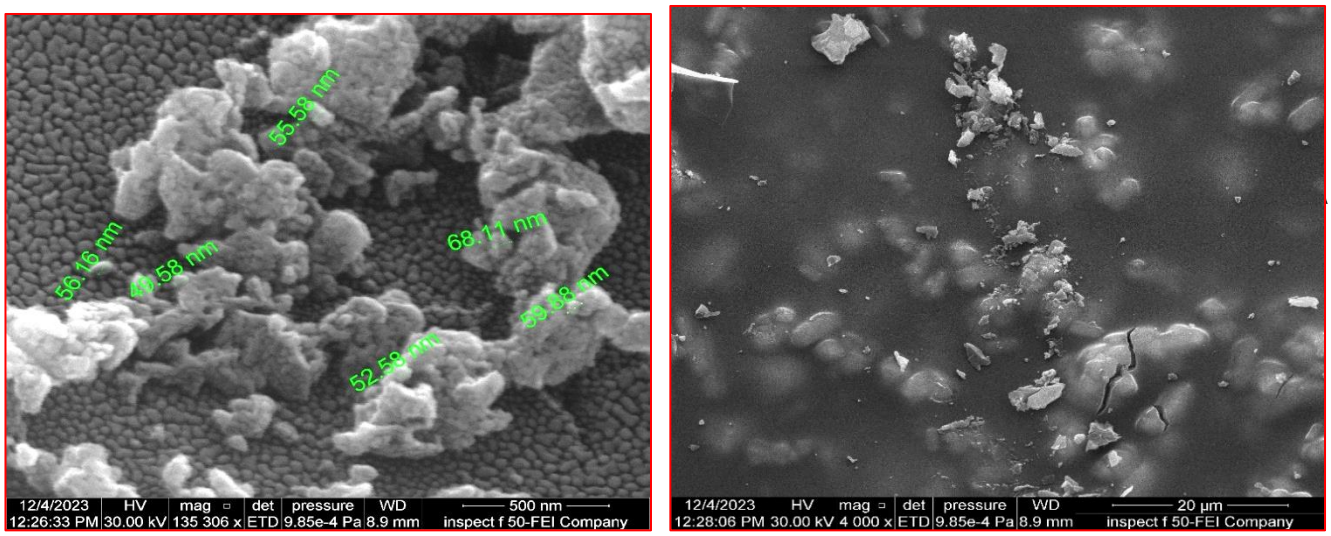

Figure (5) Shows images of the sample Fe NPs prepared by Bavarian bassiana fungus.

3.5. FTIR analyses of FeNPs

Fourier transform infrared spectroscopy (FT-IR) is an effective tool used to identify the functional groups present in the materials prepared in the current work. The vibration modes of the chemical bonds present in each of the iron oxide nanoparticle solution of the prepared sample were analyzed, in addition to the importance of studying the chemical bonds of the fungal extract used in the

preparation of Beauveria bassiana fungus. The functional groups were recorded in the range (3900-400)cm^{-1} as shown in Figure (6). The most important of these regions is the first region that lies between (700-1000)cm^{-1} which belongs to the active bond (Metal - Oxide) in which the peak is located in a fixed position. As for the second region at the range (1132)cm^{-1} , it belongs to the ether groups and the compounds that belong to them, such as epoxides, acetals and ketals (C-O-C).The third peak is at (1665) $cm^{-1}$where the fourth peak is due to the carbonyl group C=O which is an unsaturated covalent group responsible for absorption and the fourth peak indicates the wide expansion at the peak located at (3485) cm^{-1} which means the presence of groups linked to hydrogen and also represents the vibrations of (O-H) alcohol or phenolic and these results confirm the presence of the fungal extract belonging to the Beauveria bassiana fungus. The vibrations of the phenolic compounds are responsible for the Interaction process with the salts of the basic material used in the preparation through electronic transitions, through which the reduction of iron ions in the iron nanoparticles was achieved under the carbonyl bonds of the extract components to absorb the phenolic compounds to reduce those ions and convert them into oxides, so all the prepared solutions were stable during the work period.

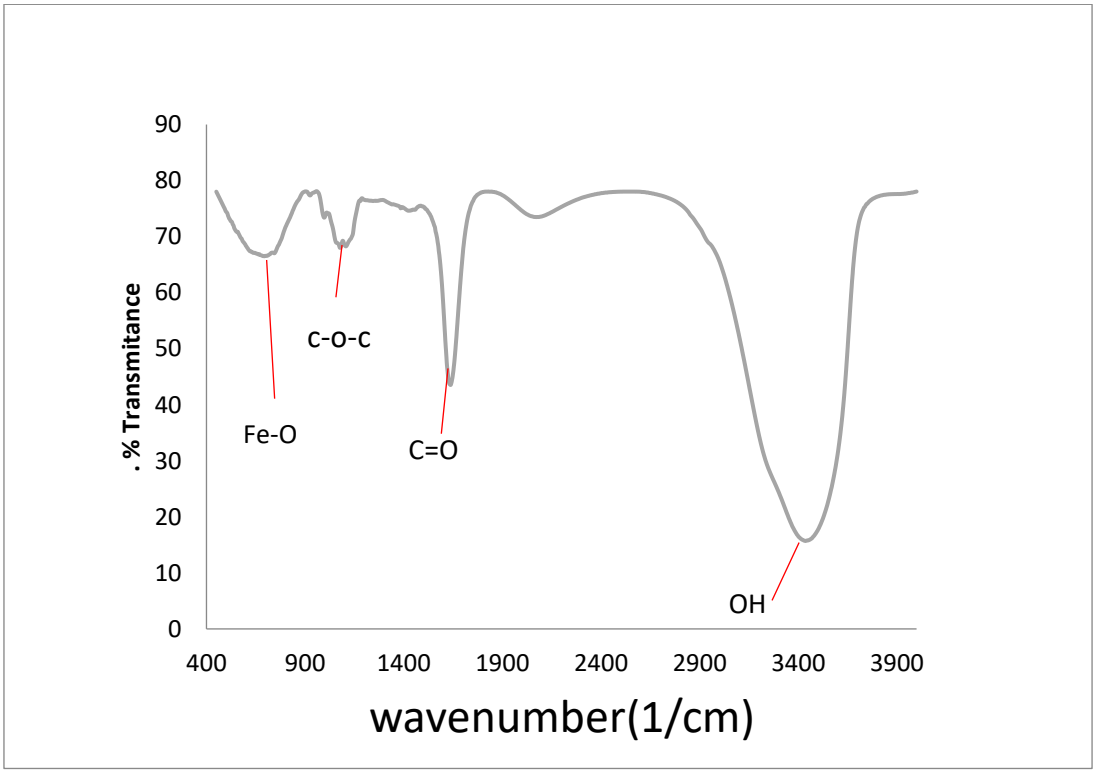

Figure (6) Shows the spectrum (FTIR) used in determining the functional clusters in the plant extract.

3.6. Optical Measurements of FeNPs

Bio-synthesized nanoparticles have visible and ultraviolet absorption spectra. The results are illustrated in Figure (7) showing the absorbance spectrum as a function of wavelength for (NPs) and the optical energy gap spectrum for the same material. The figure shows that the absorbance gradually decreases as we approach the visible light region, starting with its peak at short wavelengths, where the surface plasmon resonance is recorded, which showed absorption at the ultraviolet wavelength at (282 nm). The absorbance is at its maximum at high energies (short wavelengths), then decreases with increasing wavelength to reach its lowest value in the visible region of the spectrum. The reason for the behavior of the absorbance spectrum in this manner is that the incident photon is less than the value of the optical energy gap of the semiconductor, and for this reason the absorbance decreases with increasing wavelength, as the value of the energy gap is (2.5 eV).

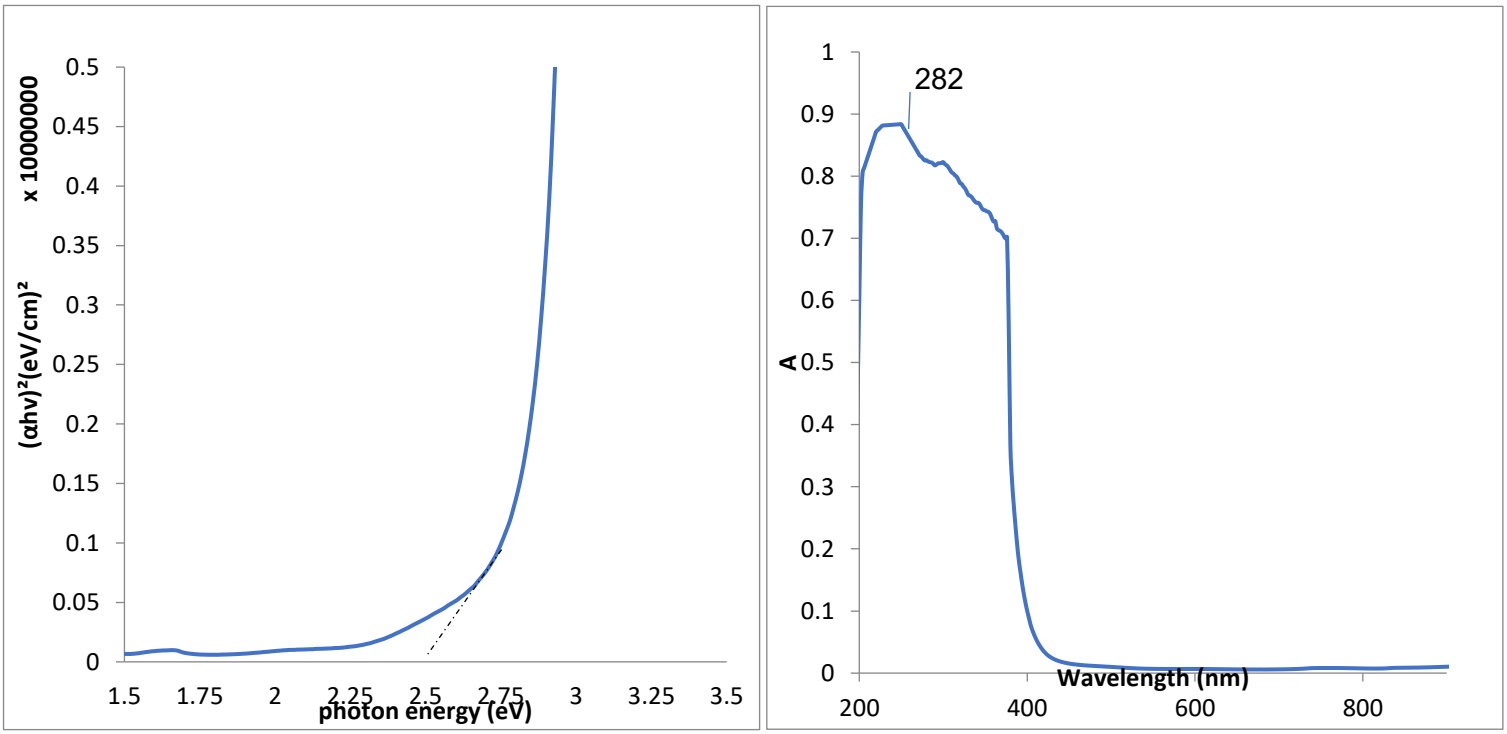

Figure (7): Absorption spectrum and optical energy gap of the prepared sample.

4.CONCLUSIONS

From the results we obtained in this work, we can conclude the following: The biosynthesis method using Beauveria bassiana fungus used in our research was suitable for preparing nanosolutions (nano iron oxide), as this method was characterized by generating nanoparticles with a crystalline structure and the morphology of these particles is in the form of irregular and dispersed particles with some crystalline structures and shapes formed by the fungal extract. It is worth noting that the (spin coater) method can produce thin films with acceptable homogeneity and regularity for studying these

solutions and is considered a fast and less costly method. Nanoparticles were successfully manufactured for the sample prepared using Beauveria bassiana fungus extract. The current study of biosynthesis using Beauveria bassiana fungus shows that the fungus extract is used as an effective oxidizing and reducing agent for the synthesis of iron oxide nanoparticles, and this method is considered clean, non-toxic and environmentally friendly for the production of iron oxide particles. UV-VIS, FTIR, XRD, AFM and SEM spectroscopic measurements showed evidence of rapid synthesis of iron oxide nanoparticles. The nanoparticles are spherical in shape and consist of B. bassiana molecules.

REFERENCES

[1]-R. W. Siegel."Synthesis and Properties of Nanophase Materials. "Materials Science and Engineering: A 168,PP(189-197) ,(1993).

[2]-N.Kumar and S. Kumbhat." Essentials in Nanoscience and Nanotechnology". John Wiley & Sons (2016).

[3]-Kamat, P. V. and Meisel, D. (2003). Nanoscience opportunities in environmental remediation. Comptes Rendus Chimie, 6 (8): 999-1007.

[4]-Kamat, P. V.; Huehn, R. and Nicolaescu, R. (2002). A “sense and shoot” approach for photocatalytic degradation of organic contaminants in water. The Journal of Physical Chemistry B, 106 (4): 788-794.

[5]- Cuenca, A. G.; Jiang, H.; Hochwald, S. N.; Delano, M.; Cance, W. G. and Grobmyer, S. R. (2006). Emerging implications of nanotechnology on cancer diagnostics and therapeutics. Cancer, 107 (3): 459-466.

[6]-Roco, C. and Bainbridge, W. S. (2002). Converging Technologies for Improving Human Performance: Nanotechnology, Biotechnology, Information Technology and Cognitive Science. Springer Science and Business Media, 486 pp.

[7]-RSRAE, N. (2004). Nanotechnologies: opportunities and uncertainties. The Royal Society and Royal Academy of Engineering, London.

[8]-Oberdörster, G.; Oberdörster, E. and Oberdörster, J. (2005). Nanotoxicology: an emerging discipline evolving from studies of ultrafine particles. Environ Health Perspect, 113 (7): 823-839.

[9]-S. Iravani, "Green synthesis of metal nanoparticles using plants," *Green Chemistry,* vol. 13, no. 10, pp. 2638-2650, 2011.

[10]-A. P. Philipse and D. Maas, "Magnetic colloids from magnetotactic bacteria: chain formation and colloidal stability," *Langmuir,* vol. 18, no. 25, pp. 9977-9984, 2002.

[11]-Vigneshwaran N, Ashtaputrea NM, Varadarajana PV, Nachanea RP, Paralikaraand KM, Balasubramanyaa RH, et al. Biological synthesis of Silvernanoparticles using the fungus Aspergillus flavus. Mater Lett 2007; 61:1413 1418.